



HAL
open science

BP-NGD Signal Integrity Application for RLC-Cable Parasitic Dispersion Reduction

T. Gu, F. Wan, B. Ravelo, P. Thakur, A. Thakur, F. Haddad, Mathieu
Guerin, W. Rahajandraibe

► **To cite this version:**

T. Gu, F. Wan, B. Ravelo, P. Thakur, A. Thakur, et al.. BP-NGD Signal Integrity Application for RLC-Cable Parasitic Dispersion Reduction. 2023 Joint Asia-Pacific International Symposium on Electromagnetic Compatibility and International Conference on ElectroMagnetic Interference & Compatibility (APEMC/INCEMIC), May 2023, Bengaluru, France. 10.1109/APEMC57782.2023.10217469 . hal-04475032

HAL Id: hal-04475032

<https://hal.science/hal-04475032v1>

Submitted on 23 Feb 2024

HAL is a multi-disciplinary open access archive for the deposit and dissemination of scientific research documents, whether they are published or not. The documents may come from teaching and research institutions in France or abroad, or from public or private research centers.

L'archive ouverte pluridisciplinaire **HAL**, est destinée au dépôt et à la diffusion de documents scientifiques de niveau recherche, publiés ou non, émanant des établissements d'enseignement et de recherche français ou étrangers, des laboratoires publics ou privés.

BP-NGD Signal Integrity Application for RLC-Cable Parasitic Dispersion Reduction

T. Gu, F. Wan, B. Ravelo
 School of Electronic & Information
 Engineering
 NUIST
 Nanjing, China
 email: {fayu.wan, taochen_gu,
 blaise.ravelo}@nuist.edu.cn

P. Thakur, A. Thakur
 Amity University Haryana
 Gurgaon, 122413 India
 email:
 {pthakur,
 athakur1}@ggn.amity.edu

F. Haddad, M. Guerin, W.
 Rahajandraibe
 AMU, CNRS, Univ. Toulon, IM2NP
 UMR7334
 13007 Marseille, France
 email: {fayrouz.haddad, mathieu.guerin,
 wenceslas.rahajandraibe}@im2np.fr

Abstract—A cable RLC-parasitic dispersion reduction by using bandpass (BP) negative group delay (NGD) circuit for signal integrity (SI) and EMC application is stressed. The theoretical formulas of uncommon BP-NGD circuit dedicated to SI enhancement versus parasitic parameters are established. The BP-NGD SI application is confirmed by AC results with circuit design under 250-MHz resonance frequency confirming dispersion reduction of magnitudes and group delays from (18-dB, 10-ns) to better than (2-dB, 2-ns). The SI improvement is validated by transient results showing input and output signal delay reduction and envelope cross correlation enhancement from 76% to 98%.

Keywords—Negative group delay (NGD), Bandpass (BP) NGD circuit, RLC-network, electric cable, dispersion effect, BP-NGD EMC application, SI improvement

I. INTRODUCTION

Cables and connectors constitute key elements for the interconnections of electric system [1-2]. Relevant EMC models of these interconnect elements are necessary to predict the electric system performance [3-5]. Accurate high frequency cable models based on transmission line (TL) theory were proposed [6-7]. The interconnect EMC parasitic affecting signal integrity (SI) degradation from cable is usually modelled by lumped and distributed RLC-networks [8-9]. To reduce the undesirable dispersion effect, one can proceed with BP-NGD equalization method [10-11]. For the case of base-band signals, low-pass type NGD equalizer must be used [12-13]. The basic specifications of NGD behavior different types were initiated by analogy with filter theory [14].

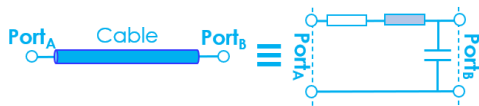


Fig. 1. Interconnect cable RLC network model configuration. The present research work elaborates AC and transient study on RLC-dispersion reduction with BP-NGD equalizer showing RF and microwave SI improvement feasibility.

II. BP-NGD THEORY ON RLC-DISPERSION REDUCTION

This section introduces the RLC-dispersion reduction BP-NGD theory established from transfer function (TF) denoted $TF_d(jf)$ and group delay (GD) $GD_d(f)$ versus frequency f .

A. Dispersion Problem Formulation

The dispersion effect is modeled by RLC equivalent circuit constituted by R_d , L_d and C_d components depicted by Fig. 2(a). The dispersion is represented by the TF_d magnitude and GD shown by Figs. 2(b) and 2(c), respectively. Under condition $L_d > R_d^2 C_d / 2$, the resonance frequency is [10]:

$$f_d = (2L_d - R_d^2 C_d)^{1/2} / (2\sqrt{2}\pi L_d C_d^{1/2}). \quad (1)$$

The dispersion magnitude and GD peaks are respectively:

$$T_d = 4L_d^2 / [R_d^2 C_d (4L_d - R_d^2 C_d)]. \quad (2)$$

$$t_0 = 2L_d / R_d. \quad (3)$$

We denote $T_1 = T_d(f_i) = T_d(f_h)$ and $t_1 = GD_d(f_h)$, and frequency band $\Delta f = f_h - f_i$. The dispersion effect is characterized by the magnitude flatness $\Delta T_d = T_1 / T_0$ and GD flatness $\Delta t_d = t_0 - t_1$.

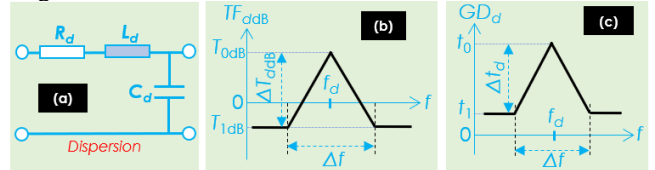


Fig. 2. Dispersion (a) equivalent circuit, (b) TF_d and (c) GD_d specifications. Knowing R_d , the dispersion model parameters are given by:

$$L_d = R_d \sqrt{\sqrt{T_d^2 - 1} (T_d + \sqrt{T_d^2 - 1})} / (2\sqrt{2}\pi f_d) \quad (4)$$

$$C_d = 1 / \left[\sqrt{2}\pi f_d R_d \sqrt{\sqrt{T_d^2 - 1} (T_d + \sqrt{T_d^2 - 1})} \right]. \quad (5)$$

B. BP-NGD Circuit Topological Description

To reduce the dispersion effect, the BP-NGD cell composed of RLC-parallel network combined to resistance, R_0 shown in Fig. 3(a) is used. The expected BP-NGD TF magnitude TF_n and GD GD_n are ideally plotted in Figs. 3(b) and 3(c), respectively. The NGD circuit is specified by its NGD center frequency, f_n , where $T_n = |TF_n(jf)|$ and $t_n = GD_n(f) < 0$, and bandwidth, Δf . The NGD cut-off frequencies must be chosen close to f_i and f_h , with $GD_n(f_i) \approx 0$ and $GD_n(f_h) \approx 0$.

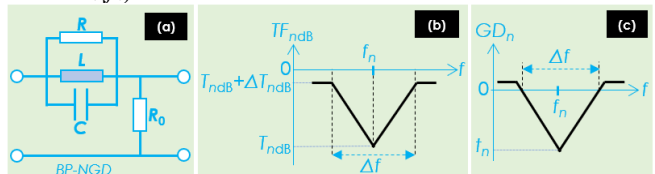


Fig. 3. BP-NGD (a) equivalent circuit, (b) TF_n and (c) GD_n specifications.

C. NGD Function Parameters Analytical Determination

The cable dispersion reduction under investigation consists originally in cascading the culprit cable and BP-NGD circuit as illustrated in Fig. 4(a). The BP-NGD equalization is aimed to operate with total TF magnitude $TF = |TF(jf)| \ll T_0$ and GD $GD(f) \ll t_0$ as presented in Fig. 4(b) and Fig. 4(c). Meanwhile, the equalized cable magnitude and GD flatness's must be improved conditions $\Delta T \ll \Delta T_d$ and $\Delta t \ll \Delta t_d$ in $[f_i, f_h]$.

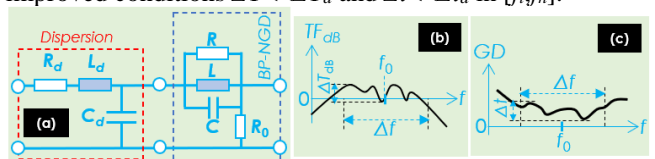


Fig. 4. TF (a) magnitude and (b) GD specifications of (c) cascaded dispersion-NGD circuit.

To achieve this dispersion reduction, the NGD parameters are calculated knowing T_0 , f_0 and R_0 by synthesis formulas:

$$R = (T_d - 1)R_0 \quad (6)$$

$$L = R_0(T_d - 1)^2 / \left[\sqrt{2\pi f_d} \sqrt{T_d \sqrt{T_d^2 - 1} + T_d^2 - 1} \right] \quad (7)$$

$$C = T_d \sqrt{T_d \sqrt{T_d^2 - 1} + T_d^2 - 1} / \left[2\sqrt{2\pi f_d} R_0 (T_d - 1)^2 \right]. \quad (8)$$

D. SI Assessment Transient Parameters

The SI performance transient parameters are referred to the comparison of input v_{in} and output v_{out} characteristics. Doing this, we can consider amplitude ratio $r = \max(v_{out}) / \max(v_{in})$. By taking the half-maximum $x = \{\text{rise, fall}\}$ instant times of input $v_{in}(t_{in}^x) = \max(v_{in}) / 2$ and output $v_{out}(t_{out}^x) = \max(v_{out}) / 2$, the signal delays are defined as $\Delta t_x = t_{out}^x - t_{in}^x$. The input and output relative correlation is equated by MATLAB® instruction $xc = \text{corrcoef}(v_{in}, v_{out})$.

III. CABLE DISPERSION REDUCTION VALIDATION

A. POC Design

The dispersion reduction POCs are designed in the schematic environment of the ADS® commercial tool from Keysight Technologies® as displayed by Figs. 5 with corresponding parameters addressed in Table I. The RLC resonant circuit inductance, L_d and capacitance, C_d , were calculated from equations (4) and (5) by fixing the value of resistor, $R_d = 10.25 \Omega$. The BP-NGD parameters were synthesized by mean of formulas (6), (7) and (8) by assuming $R_0 = 50 \Omega$.

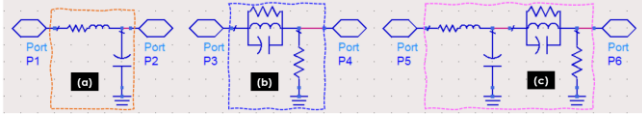


Fig. 5. (a) Dispersion, (b) BP-NGD and (c) equalized circuit ADS® POCs.

TABLE I
POC DISPERSION AND PARAMETERS

Dispersion	Parameter	$f_d=0.25\text{GHz}$	$T_d=18\text{dB}$	$t_d=10\text{ns}$
	RLC-model	$R_d=10.25\Omega$	$L_d=51.2\text{nH}$	$C_d=8.24\text{pF}$
BP-NGD parameter		$R=362\Omega$	$L=21.6\text{nH}$	$C=19.5\text{pF}$

B. Dispersion Reduction AC Validation Results

The POC AC analysis was carried in the frequency band delimited from $f_{min}=0.15$ GHz to $f_{max}=0.35$ GHz. The significant flatness of magnitudes and GDs of TF, respectively displayed in Figs. 6(a) and 6(b), reveals the effectiveness of the dispersion reduction. The calculated (“ TF_{Dc} ,” “ TF_{Nc} ” and “ TF_{DNc} ”) and simulated (“ TF_{Ds} ,” “ TF_{Ns} ” and “ TF_{DNs} ”) responses, plotted in solid and dotted curves, respectively are in excellent agreement. The dispersion, NGD and total TF responses, denoted TF_D , TF_N and TF_{DN} , respectively are plotted in solid black, red dashed and blue dotted curves, respectively. Table II summarizes the magnitude and GD at $f_d=f_h$. Thanks to the BP-NGD function with cut-off frequencies, f_l and f_h under about 80 MHz NGD bandwidth, obvious reduction of resonance magnitude, TF_D , is observed compared to TF , and also the GD, GD_D , compared to GD in the NGD frequency band.

TABLE II
NGD AND DISPERSION SPECIFICATIONS

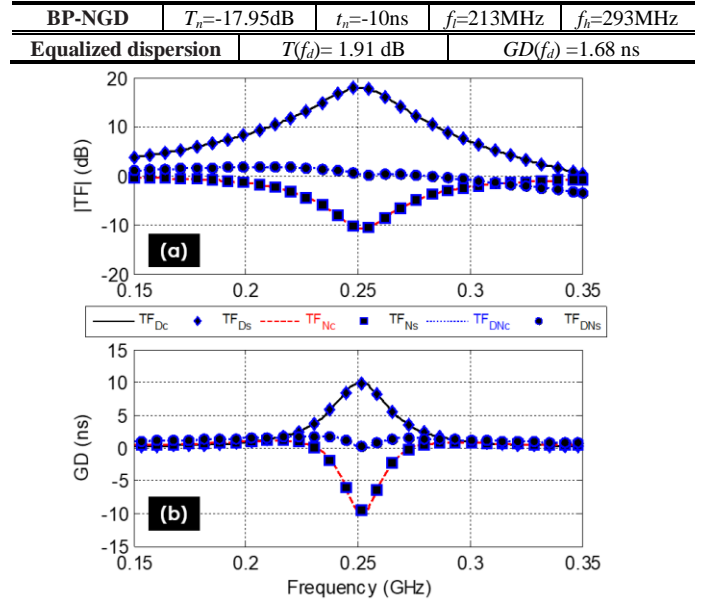


Fig. 6. Comparisons of calculated and simulated (a) magnitudes and (b) GDs. As expected, TF , of the equalized dispersion presents a better flatness.

C. BP-NGD Transient Signature

To highlight the BP-NGD meaning, input pulse signal v_{in} of circuit proposed in Fig. 5(b) modulated by 1 V amplitude modulating since carrier frequency f_d was considered. The test input signal spectrum belongs also to the NGD bandwidth with 60 ns period under transient analysis within 100 ns duration the time window. Fig. 7(a) and Fig. 7(b) show the plots of the input and BP-NGD output transient signals v_{in} and v_{NGD} . As explained by normalized envelopes $\text{Env}[v_{in}]$ (plotted in black solid line) and $\text{Env}[v_{NGD}]$ (plotted in blue solid line) compared in Fig. 7(c), despite the slight ripple distortion, the BP-NGD signature is confirmed by time-advance effect.

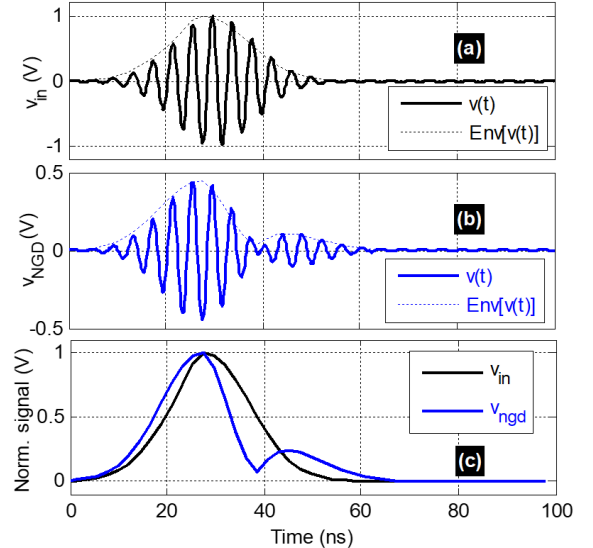


Fig. 7. Transient plot results illustrating BP-NGD signature.

D. Transient Results Showing Dispersion Reduction Implying SI Improvement

In addition to the previous AC analysis, the previously considered input signal v_{in} was injected to the dispersion and equalized circuits described in Fig. 5(a) and Fig. 5(b). Fig. 8(b) and Fig. 8(c) show the plots of the dispersion and equalized signals v_d and v_{eq} . The associated signal envelopes

$\text{Env}[v_d]$ (plotted in red dashed line) and $\text{Env}[v_{eq}]$ (plotted in pink solid line) compared to $\text{Env}[v_{in}]$ are plotted in Fig. 9(a).

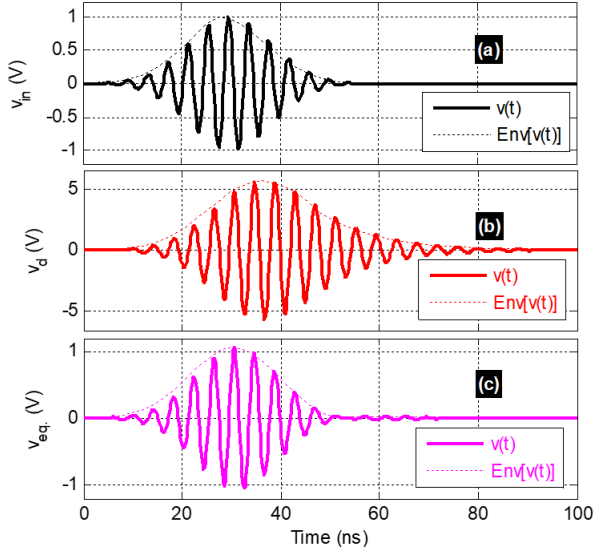


Fig. 8. (a) Input, (b) dispersion and (c) equalized transient signal results. It can be seen that v_d is literally distorted by showing wider time width pulse. This distortion effect is significantly reduced by referring to v_{eq} shown in Fig. 9(b). We remark that the original and BP-NGD equalized signals present a highly improved correlation coefficient and signal delay reduction as summarized in Table III.

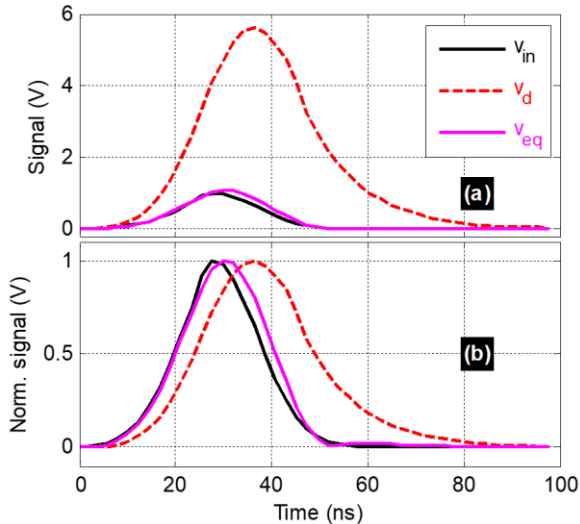


Fig. 9. Comparison of input, dispersion and equalized (a) natural and (b) normal envelopes.

TABLE III
COMPARISON OF DISPERSION AND EQUALIZED SI PARAMETERS

Output/input SI parameters	xc	Δt_{rise}	Δt_{fall}	r
Dispersion	76%	5 ns	10 ns	15 dB
BP-NGD equalization	98%	0.5 ns	2 ns	1.1 dB

IV. CONCLUSION

A SI application of uncommon BP-NGD circuit for

reducing interconnect cable RLC-dispersion is studied. The BP-NGD circuit design equalization method is formulated. Relevant AC and transient results confirm the BP-NGD dispersion reduction method effectiveness for EMC and SI engineering.

ACKNOWLEDGMENT

This research work was supported in part by NSFC under Grant 61971230, and in part by Jiangsu Distinguished Professor program and Six Major Talents Summit of Jiangsu Province (2019-DZXX-022), and in part by the Postgraduate Research & Practice Innovation Program of Jiangsu Province under Grant SJKY19_0974.

REFERENCES

- [1] F. H. G. Hudson, S. L. Stronach, W. Derr, W. A. Johnson, L. K. Warne, and R. E. Jorgenson, "Cable test system upgrade-Coaxial cable/connector model validation experiments," Internal Sandia Test Report, FY2000/2001.
- [2] O. Maurice, Elements of Theory for Electromagnetic Compatibility and Systems, Bookelis, Aix en Provence, France, 2017.
- [3] O. Maurice, "Proposal of a method for real cables EMC modeling," White paper, 2008, pp. 1-8, HAL Id: hal-00311651, <https://hal.archives-ouvertes.fr/hal-00311651>
- [4] S. Campione, L. K. Warne, R. S. Coats, W. L. Langston, L. I. Basilio, and W. A. Johnson, "A first principles cable braid electromagnetic penetration model," PIER B, vol. 66, pp. 63–89, Jan. 2016.
- [5] R. Otin, J. Verpoorte, and H. Schippers, "Finite element model for the computation of the transfer impedance of cable shields," IEEE Trans. Electromagn. Compat., vol. 53, no. 4, pp. 950–958, Nov. 2011.
- [6] R. Casagrande, O. Maurice and A. Reineix, "High frequency bundles modeling," in Proc. of Int. Symp. EMC (EMC EUROPE), 2013, Brugge, Belgium, 2-6 Sept. 2013, pp. 264-269.
- [7] J. H. Kim, D. Oh, and W. Kim, "Accurate characterization of broadband multiconductor transmission lines for high-speed digital systems," IEEE Tran. Adv. Packag., vol. 33, no. 4, pp. 857-867, Nov. 2010.
- [8] S. Roy and A. Dounavis, "RLC interconnect modeling using delay algebraic equations," in Proc. IEEE Circuits Syst. Workshop, Richardson, TX, USA, Oct. 4–5, 2009, pp. 1-4.
- [9] T. Eudes, B. Ravelo, and A. Louis, "Experimental validations of a simple PCB interconnect model for high-rate signal integrity," IEEE Trans. Electromagn. Compat., vol. 54, no. 2, pp. 397–404, Apr. 2012.
- [10] B. Ravelo, F. Wan, J. Nebhen, W. Rahajandraibe, S. Lall ch re, "Resonance Effect Reduction with Bandpass Negative Group Delay Fully Passive Function," IEEE TCAS II: Express Briefs, vol. 68, pp. 2364-2368, (2021).
- [11] B. Ravelo, S. Lall ch re, W. Rahajandraibe, and F. Wan, "Electromagnetic Cavity Resonance Equalization with Bandpass Negative Group Delay," IEEE TEMC, vol. 63, pp. 1248-1257, (2021).
- [12] B. Ravelo, W. Rahajandraibe, Y. Gan, F. Wan, N. M. Murad and A. Douy re, "Reconstruction Technique of Distorted Sensor Signals with Low-Pass NGD Function," IEEE Access, Vol. 8, No. 1, Dec. 2020, pp. 92182-92195.
- [13] B. Ravelo, "Recovery of Microwave-Digital Signal Integrity with NGD Circuits", Photonics and Optoelectronics (P&O), Vol. 2, No. 1, Jan. 2013, pp. 8-16.
- [14] B. Ravelo, "Similitude between the NGD function and filter gain behaviours," Int. J. Circ. Theor. Appl., vol. 42, no. 10, Oct. 2014, pp. 1016-1032.